

# Structural—Functional Role of Chloride in Photosystem II

Ivan Rivalta,<sup>\*,†</sup> Muhamed Amin,<sup>‡</sup> Sandra Luber,<sup>†</sup> Serguei Vassiliev,<sup>§</sup> Ravi Pokhrel,<sup>†</sup> Yasufumi Umena,<sup>||</sup> Keisuke Kawakami,<sup>⊥</sup> Jian-Ren Shen,<sup>@</sup> Nobuo Kamiya,<sup>⊥</sup> Doug Bruce,<sup>\*,§</sup> Gary W. Brudvig,<sup>\*,†</sup> M. R. Gunner,<sup>\*,‡</sup> and Victor S. Batista<sup>\*,†</sup>

<sup>†</sup>Department of Chemistry, Yale University, New Haven, Connecticut 06520-8107, United States

<sup>‡</sup>Department of Physics, J-419, City College of New York, 138th Street, Convent Avenue, New York, New York 10031, United States

<sup>§</sup>Department of Biological Sciences, Brock University, 500 Glenridge Avenue, St. Catharines, ON L2S 3A1, Canada

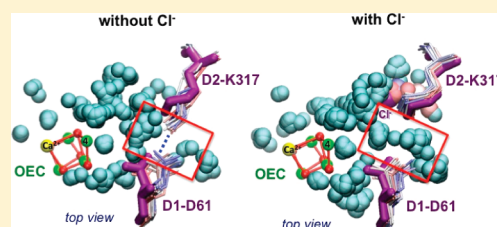
<sup>||</sup>Institute for Protein Research, Osaka University, 3-2 Yamadaoka, Suita-shi, Osaka 565-0871, Japan

<sup>⊥</sup>Department of Chemistry, Graduate School of Science, and The OCU Advanced Research Institute for Natural Science and Technology (OCARINA), Osaka City University, Sumiyoshi, Osaka 558-8585, Japan

<sup>@</sup>Division of Bioscience, Graduate School of Natural Science and Technology/Faculty of Science, Okayama University, 1-1, Naka 3-chome, Tsushima, Okayama 700-8530, Japan

**S** Supporting Information

**ABSTRACT:** Chloride binding in photosystem II (PSII) is essential for photosynthetic water oxidation. However, the functional roles of chloride and possible binding sites, during oxygen evolution, remain controversial. This paper examines the functions of chloride based on its binding site revealed in the X-ray crystal structure of PSII at 1.9 Å resolution. We find that chloride depletion induces formation of a salt bridge between D2-K317 and D1-D61 that could suppress the transfer of protons to the lumen.



Light-driven oxygen evolution in photosynthetic organisms is catalyzed by photosystem II (PSII), an ~350 kDa complex of 20 proteins embedded in the thylakoid membranes of green plant chloroplasts, or internal membranes of cyanobacteria.<sup>1</sup> Dioxygen evolves from the oxidation of water catalyzed by the oxygen-evolving complex (OEC) of PSII, a Mn<sub>4</sub>CaO<sub>5</sub> cluster embedded in protein subunit D1. This catalytic cluster is of great biological and technological interest because it is composed of inexpensive earth-abundant metals (e.g., Mn and Ca) and has an efficient turnover number as high as 50 dioxygen molecules per second for direct solar-driven water oxidation that is yet to be matched by artificial systems (Figure 1).<sup>2</sup> Recent breakthroughs in X-ray crystallography<sup>1</sup> provide evidence of a cuboidal cluster MnCaMn<sub>3</sub>, similar to previous proposals,<sup>3–5</sup> with a “dangling” Mn bound to the CaMn<sub>3</sub> cube, as well as information about the position of Cl<sup>−</sup> cofactor ions.<sup>1,6</sup> These breakthroughs open an opportunity for studies of structure–function relations that might provide fundamental insight into the potential role of Cl<sup>−</sup> in the reaction mechanism. The Cl<sup>−</sup> concentration is regulated very effectively under a variety of conditions in chloroplasts,<sup>7,8</sup> and it is well-known that Cl<sup>−</sup> depletion suppresses O<sub>2</sub> evolution,<sup>9–11</sup> although the specific roles played by Cl<sup>−</sup> in the underlying catalytic process remain to be established at the molecular level.<sup>12,13</sup> This paper addresses the potential influence of Cl<sup>−</sup> binding on the hydrogen bonds of amino acid residues in close contact with the OEC that might facilitate fundamental processes that are essential for oxygen evolution, including water gating and the transfer of protons to the lumen.

The catalytic mechanism of evolution of O<sub>2</sub> by oxidation of water in PSII is driven by solar light absorption. The absorbed photon energy is transferred to the reaction center where it is used to oxidize a chlorophyll *a* species called P680, forming the radical-pair state P680<sup>++</sup>Q<sub>A</sub><sup>•−</sup> by reducing the protein-bound quinone cofactor, Q<sub>A</sub>. The oxidizing power accumulated in P680<sup>++</sup> is used to oxidize Y<sub>Z</sub>, which in turn oxidizes the OEC through a series of S states, with S<sub>0</sub> and S<sub>4</sub> being the most reduced and oxidized states, respectively. The S<sub>4</sub> state has enough oxidizing potential to oxidize water, regenerating the S<sub>0</sub> state for the next catalytic turnover cycle. Experimental evidence shows that oxidation-state transitions beyond the S<sub>2</sub> state are suppressed upon Cl<sup>−</sup> depletion or competitive binding of acetate in place of Cl<sup>−</sup>.<sup>14,15</sup> However, the specific functional—structural roles of Cl<sup>−</sup> during the catalytic cycle have yet to be established. An early hypothesis of Cl<sup>−</sup> ions bridging Mn atoms in the OEC core<sup>8</sup> was ruled out by X-ray absorption spectroscopy experiments<sup>16,17</sup> in the early 1990s, but the functional role of Cl<sup>−</sup> remained obscure. Fundamental information about structural characterization of the PSII protein complex<sup>18</sup> and the OEC<sup>5</sup> was achieved with the beginning of the “solid structural era” of PSII.<sup>19</sup> In spite of that, the characterization of Cl<sup>−</sup> binding sites in PSII by X-ray crystallography has remained elusive until very recently.<sup>1,6,12,13,20</sup> The absence of crystallographic information about Cl<sup>−</sup> positions around the OEC triggered a series of studies

**Received:** May 4, 2011

**Revised:** June 14, 2011

**Published:** June 16, 2011

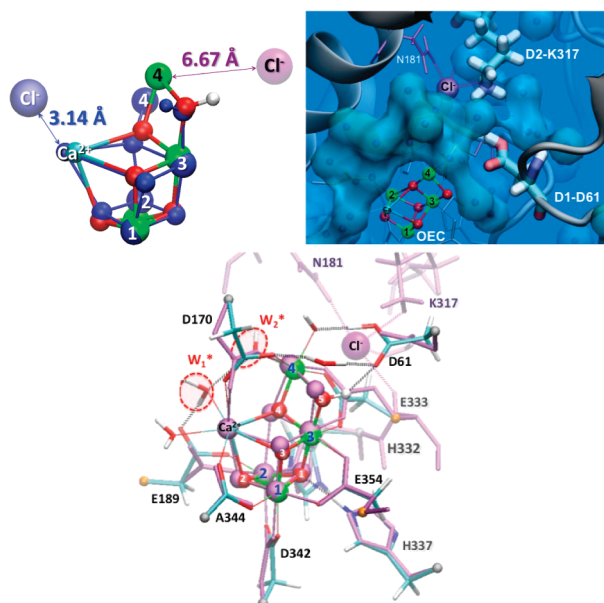


**Figure 1.** Position of  $\text{Cl}^-$  relative to the OEC in the X-ray structure of PSII at 1.9 Å (colored ball and sticks) and the 2006 DFT-QM/MM model (blue ball and sticks), aligned to minimize the root-mean-square deviation of Mn1, Mn2, Mn3, and  $\text{Ca}^{2+}$  (top left). Waters modeled in the 1.9 Å structure (gray spheres) next to the  $\text{Cl}^-$ , the OEC, and residues D1-D61 and D2-K317 (top right). Ligation of the OEC defined for MD and MCCE simulations, according to our new  $\text{S}_1$ -state DFT-QM/MM model (colored ball and sticks) (bottom) (see the Supporting Information and DOI 10.1021/bi200681q). The X-ray structure is shown in light purple for comparison.

that aimed to reveal the binding sites of chloride in the proximity of the OEC and its functional role in PSII.<sup>9,10,17,21–28</sup> Some of the proposed binding sites involved ligation of chloride to manganese.<sup>9,10,21–25</sup> Other models suggested association with amino acid residues in the Mn coordination shell,<sup>17,26</sup> and its potential functional role in the regulation of the redox potentials of the  $\text{MnCaMn}_3$  cluster,<sup>27</sup> participation in hydrogen bond networks,<sup>3,28,29</sup> and activation of the substrate water.<sup>28</sup> Recent X-ray crystallographic studies of bromide-substituted and iodine-substituted PSII revealed the presence of two binding sites for halide anions in the proximity of the OEC.<sup>12,13</sup> This experimental evidence suggested that bromide (and by analogy chloride) can facilitate the access of substrate water and remove protons from the OEC and supported the idea of a proton-relay network constituted by chloride and charged amino acid side chains.<sup>29</sup> The position of chloride determined in the crystal structure of cyanobacterial photosystem II<sup>20</sup> was found to match one of the two binding sites determined for bromide. In the most recent X-ray structure of *Thermosynechococcus vulcanus* PSII at 1.9 Å resolution,<sup>1</sup> two chloride binding sites near the OEC were finally resolved.

In one binding site (BS1),  $\text{Cl}^-$  is bound to the NH groups of D1-N338, D1-F339, and CP43-E354 backbones, 7.40 Å from the OEC [i.e., from Mn(1)]. Here,  $\text{Cl}^-$  is not directly interacting with a counterion, and the closest protonatable residue is D1-H337 [at 6.20 Å (see Figure S2 of the Supporting Information)], indicating that  $\text{Cl}^-$  located in this binding pocket should not affect the protonation state of amino acid residues close to the OEC. In the second binding pocket (BS2),  $\text{Cl}^-$  is located in the proximity of the positively charged D2-K317 side chain [6.67 Å from Mn(4) (see Figure 1)],<sup>1,12,13</sup> interacting with the backbone

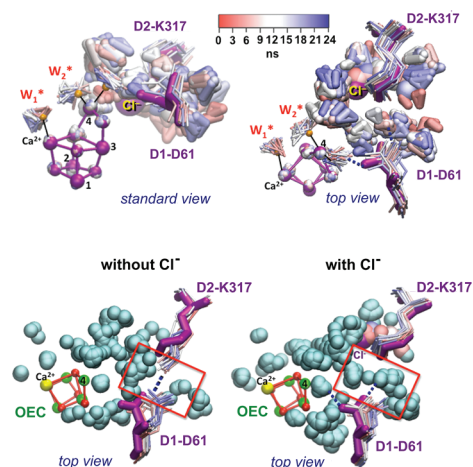


**Figure 2.** Top panel: Superposition of instantaneous configurations along MD simulations, including  $\text{H}_2\text{O}$  molecules ( $\text{W}_1^*$  and  $\text{W}_2^*$ ),  $\text{Cl}^-$ , residues D1-D61 and D2-K317, and bound waters (triangles colored from red to blue for 0–24 ns). Bottom panel: A salt bridge is formed between K317 and D61 (left, without  $\text{Cl}^-$ ) and is interrupted by water (right, with  $\text{Cl}^-$ ). The water oxygen atoms are colored cyan. The X-ray structure is colored purple.

of D1-E333 and the polar side chain of D1-N181 (see Figure S2). The most recent X-ray structure revealed that the D1-D61 side chain occupies a critical position between the  $\text{MnCaMn}_3$  cluster of OEC and this chloride-binding pocket. Therefore, we focus on the potential influence of chloride binding on the protonation state of D1-D61, which can be modified by hydrogen bonding and electrostatic interactions with nearby amino acid residues, including D2-K317 and D1-E333. These fundamental interactions might play important roles in water gating and proton transfer mechanisms because D1-D61 is the first residue leading from the OEC to the luminal side of the membrane (see Figure 1, top right). Moreover, oxygen release in D61N and D61A point mutants from *Synechocystis* sp. PCC 6803 is slowed by a factor of 8–10 [compared to that of the wild type (WT)], with flash-spectrophotometric measurements indicating that residue D1-D61 interacts directly with the  $\text{MnCaMn}_3$  unit and selectively affects the redox potentials of the OEC cluster.<sup>32</sup> Interestingly, the D61E mutation in the cyanobacterium does not change the oxygen release of PSII with respect to WT, suggesting that a charged (and protonatable) residue at position 61 is crucial for the efficiency of photosynthetic function.

In this work, we analyze the effect of chloride binding on specific hydrogen bonding interactions by using molecular dynamics (MD)<sup>33</sup> and Monte Carlo (MC) within multiconformer continuum electrostatics (MCCE).<sup>34</sup> MCCE binding constants show the strong affinity of  $\text{Cl}^-$ <sup>35</sup> for both sites with BS2 estimated to bind  $\approx 10$  kcal/mol tighter than BS1. The  $\text{pK}_a$  of D1-D61 is estimated to be lower than 5 when both  $\text{Cl}^-$  atoms are bound. In BS1, the interactions between  $\text{Cl}^-$  and the backbones of the D1 C-terminal loop and CP43 polypeptide appear to stabilize the structural conformation by which D1-D342, D1-A344, and CP43-E354 are bound to the OEC (see Figure S3), stabilizing the Mn cofactor in PSII. The higher binding affinity for  $\text{Cl}^-$  in BS2 with respect to BS1 is due to its interaction with the positively charged D2-K317 side chain. Moreover,  $\text{Cl}^-$  binding in BS2 could affect the protonation state of amino acid residues close to the OEC, such as D1-D61, playing a role in the proton transfer mechanism.

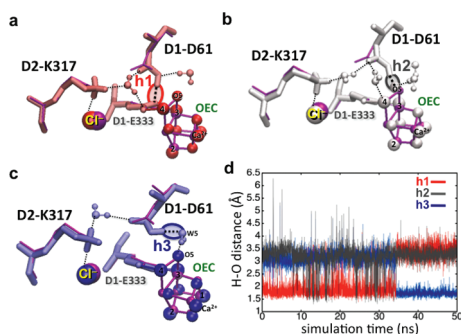


**Figure 3.** (a–c) Representative configurations of H-bonds between protonated D1-D61 and polar moieties at 1 ns (red, a), 22 ns (gray, b), and 48 ns (blue, c), including interactions with D1-E333 (h1), the  $\mu$ -oxo bridge linking Mn(3) and Mn(4) (h2), and a water moiety H-bonded to the  $\mu$ -oxo bridge (h3). The X-ray structure is colored magenta. (d) H-Bond distances for h1–h3, along a 50 ns MD simulation.

We find evidence of significant changes in the interactions of the side chain of D1-D61 induced by chloride depletion (Figure 2). Specifically, MC and MD simulations predict that  $\text{Cl}^-$  depletion induces formation of a salt bridge between the negatively charged carboxylate group of D1-D61 and the positively charged side chain of D2-K317 (Figure 2, left). Thus as a consequence,  $\text{Cl}^-$  depletion would stabilize an inactive configuration of charged amino acid side chains in the hydrogen bonding network close to the  $\text{MnCaMn}_3$  cluster, where D1-D61 is unable to extract protons from the OEC. We observed that the formation of the D1-D61–D2-K317 salt bridge is independent of the protonation state of the  $\mu$ -oxo linking Mn(3) and Mn(4). The absence of  $\text{Cl}^-$  could, thus, affect the deprotonation of the different S states in the Kok cycle.

In contrast, in the presence of  $\text{Cl}^-$ , the carboxylate group of the anionic D1-D61 moves and is often hydrogen bonded to a water ligand of the dangling Mn as well as to a water in contact with the D2-K317  $\text{NH}_3^+/\text{Cl}^-$  ion pair (Figure 2, right). MD simulations show thermal fluctuations in the position of  $\text{Cl}^-$ , correlated to fluctuations in the configurations of surrounding water moieties and side chains of D2-K317 and D1-D61 (see Figure 2). MC analysis also shows multiple positions of the D61 side chain (see Figure S5). However, partial solvation screens the electrostatic interactions between the negatively charged carboxylate group of D1-D61 and the proximal D2-K317  $\text{NH}_3^+/\text{Cl}^-$  ion pair, preventing D1-D61 from displacing  $\text{Cl}^-$  and interacting directly with D2-K317. Both MCCE electrostatic analysis and MD simulations show that the protein could stabilize the protonated form of D1-D61. This is due to desolvation of D1-D61 by burial in the protein and its proximity to nearby anionic species, including the carboxylate group of D1-E333 and the  $\mu$ -oxo bridge linking Mn(3) and Mn(4). MD simulations show evidence of specific hydrogen bonding interactions for the neutral form of D1-D61 (Figure 3). Figure 3d shows that thermal fluctuations allow the hydroxyl group of D1-D61 to switch hydrogen bonds between these polar species on the nanosecond time scale. The relative stability of these three types of hydrogen bonds is also manifested by their corresponding lifetimes. Hydrogen bonds with D1-E333 (h1) or with a water moiety H-bonded to the  $\mu$ -oxo linking Mn(3) and Mn(4) (h3) are very stable, while the H-bond with the  $\mu$ -oxo bridge (h2) is observed only transiently (see Figure 3). These relative lifetimes suggest that a protonated state of the  $\mu$ -oxo bridge would be destabilized

by thermal fluctuations of the carboxylate group of D1-D61, with proton transfer from the OEC to D1-D61 leading to formation of h1 or h3. Therefore, different conformations, protonation states, and hydrogen bonding of D1-D61 might be observed during the S-state cycle, supporting the idea that conformational changes of D1-D61 coupled with  $\text{Cl}^-$  might be an essential aspect of the OEC deprotonation mechanism.<sup>36</sup> MCCE analysis shows that a hydrogen bond can be made between the anionic D1-D61 and terminal water bound to Mn(4) or between the protonated D1-D61 and a terminal hydroxide bound to Mn(4), supporting the notion that this could be a site for proton transfer. Interestingly, MD simulations of  $\text{Cl}^-$ -depleted PSII indicated that, in the presence of a neutral D1-D61, the positively charged D2-K317 is attracted to the negatively charged side chain, D1-D65, which is, however, too distant to form an alternative salt bridge. This supports the idea that the main effect of  $\text{Cl}^-$  depletion is to alter the functional role of D1-D61 as a “molecular gate” for the transfer of protons from the OEC core to the lumen by allowing D1-D61 to form a stable (and catalytically inactive) salt bridge with D2-K317. We propose that a primary role of  $\text{Cl}^-$  as an allosteric regulator of PSII is to stabilize a configuration of charged side chains close to the OEC that favors a flexible conformation of the basic center (D1-D61), assisting the proton abstraction mechanism from the OEC core. We considered the possibility of having the protonated form of D1-D61 hydrogen bonded to  $\text{Cl}^-$ . However, MD simulations initialized by placing  $\text{Cl}^-$  between D2-K317 and D1-D61 show fast diffusion of  $\text{Cl}^-$  back into the  $\text{Cl}^-$  binding pocket found in the X-ray structure in <3 ns, 6.7 Å from Mn(4) (see Figure S4). Here the backbone of D1-E333, the polar side chain of N181, and two water molecules provide more favorable H-bonding interactions (see Figure S1b).

In summary, MD and MC simulations of PSII both show evidence of specific electrostatic interactions between  $\text{Cl}^-$  and essential amino acid residues in close contact with the OEC. We conclude that  $\text{Cl}^-$  depletion induces formation of a salt bridge between D2-K317 and D1-D61 that could hinder the transfer of protons to the lumen, as previously proposed.<sup>36</sup> Further work is required to establish the detailed mechanism of proton transfer in PSII.

## ■ ASSOCIATED CONTENT

**S Supporting Information.** Description of computational methods and structural models. This material is available free of charge via the Internet at <http://pubs.acs.org>.

## ■ AUTHOR INFORMATION

### Corresponding Authors

\*E-mail: [gary.brudvig@yale.edu](mailto:gary.brudvig@yale.edu), [gunner@sci.ccnny.cuny.edu](mailto:gunner@sci.ccnny.cuny.edu), [ivan.rivalta@yale.edu](mailto:ivan.rivalta@yale.edu), [dbruce@brocku.ca](mailto:dbruce@brocku.ca), or [victor.batista@yale.edu](mailto:victor.batista@yale.edu). Phone: (203) 432-6672. Fax: (203) 432-6144.

### Funding Sources

We acknowledge financial support from the Division of Chemical Sciences, Geosciences, and Biosciences, Office of Basic Energy Sciences, U.S. Department of Energy (DE-SC 0001423). V.S.B. acknowledges supercomputer time from National Energy Research Scientific Computing and support from National Institutes of Health (NIH) grants GM84267 and GM043278 for the development of methods and models implemented in this study. G.W.B. acknowledges support from NIH Grant GM32715.



## REFERENCES

- (1) Umena, Y., Kawakami, K., Shen, J.-R., and Kamiya, N. (2011) *Nature* 473, 55–60.
- (2) Blankenship, R. E. (2002) *Molecular Mechanisms of Photosynthesis*, Blackwell Science, Oxford, U.K.
- (3) Sproviero, E. M., Gascon, J. A., McEvoy, J. P., Brudvig, G. W., and Batista, V. S. (2006) *J. Chem. Theory Comput.* 2, 1119–1134.
- (4) Sproviero, E. M., Shinopoulos, K., Gascon, J. A., McEvoy, J. P., Brudvig, G. W., and Batista, V. S. (2008) *Philos. Trans. R. Soc. London, Ser. B* 363, 1149–1156.
- (5) Ferreira, K. N., Iverson, T. M., Maghlaoui, K., Barber, J., and Iwata, S. (2004) *Science* 303, 1831–1838.
- (6) Kawakami, K., Umena, Y., Kamiya, N., and Shen, J.-R. (2011) *J. Photochem. Photobiol., B* 104, 9–18.
- (7) Demmig, B., and Winter, K. (1983) *Planta* 159, 66–76.
- (8) Critchley, C. (1985) *Biochim. Biophys. Acta* 811, 33–46.
- (9) Sandusky, P. O., and Yocum, C. F. (1984) *Biochim. Biophys. Acta* 766, 603–611.
- (10) Brudvig, G. W., Beck, W. F., and de Paula, J. C. (1989) *Annu. Rev. Biophys. Biochem.* 18, 25–46.
- (11) Popelkova, H., and Yocum, C. F. (2007) *Photosynth. Res.* 93, 111–121.
- (12) Murray, J. W., Maghlaoui, K., Kargul, J., Ishida, N., Lai, T. L., Rutherford, A. W., Sugiura, M., Boussac, A., and Barber, J. (2008) *Energy Environ. Sci.* 1, 161–166.
- (13) Kawakami, K., Umena, Y., Kamiya, N., and Shen, J. R. (2009) *Proc. Natl. Acad. Sci. U.S.A.* 106, 8567–8572.
- (14) Kühne, H., Szalai, V. A., and Brudvig, G. W. (1999) *Biochemistry* 38, 6604–6613.
- (15) Wincencjusz, H., van Gorkom, H. J., and Yocum, C. F. (1997) *Biochemistry* 36, 3663–3670.
- (16) Yachandra, V. K., DeRose, V. J., Latimer, M. J., Mukerji, I., Sauer, K., and Klein, M. P. (1993) *Science* 260, 675–679.
- (17) Haumann, M., Barra, M., Loja, P., Loscher, S., Krivanek, R., Grundmeier, A., Andréasson, L.-E., and Dau, H. (2006) *Biochemistry* 45, 13101–13107.
- (18) Zouni, A., Witt, H. T., Kern, J., Fromme, P., Krauss, N., Saenger, W., and Orth, P. (2001) *Nature* 409, 739–743.
- (19) Rhee, K. H. (2001) *Annu. Rev. Biophys. Biomol. Struct.* 30, 307–328.
- (20) Guskov, A., Kern, J., Gabdulkhakov, A., Broser, M., Zouni, A., and Saenger, W. (2009) *Nat. Struct. Mol. Biol.* 16, 334–342.
- (21) Hureau, C., Blondin, G., Charlot, M. F., Philouze, C., Nierlich, M., Cesario, M., and Anxolabehere-Mallart, E. (2005) *Inorg. Chem.* 44, 3669–3683.
- (22) Yachandra, V. K., Sauer, K., and Klein, M. P. (1996) *Chem. Rev.* 96, 2927–2950.
- (23) Pecoraro, V. L., Baldwin, M. J., Caudle, M. T., Hsieh, W. Y., and Law, N. A. (1998) *Pure Appl. Chem.* 70, 925–929.
- (24) Vrettos, J. S., Limburg, J., and Brudvig, G. W. (2001) *Biochim. Biophys. Acta* 1503, 229–245.
- (25) Britt, R. D., Campbell, K. A., Peloquin, J. M., Gilchrist, M. L., Aznar, C. P., Dicus, M. M., Robblee, J., and Messinger, J. (2004) *Biochim. Biophys. Acta* 1655, 158–171.
- (26) Hasegawa, K., Kimura, Y., and Ono, T. A. (2002) *Biochemistry* 41, 13839–13850.
- (27) Boussac, A., and Rutherford, A. W. (1994) *J. Biol. Chem.* 269, 12462–12467.
- (28) McEvoy, J. P., and Brudvig, G. W. (2004) *Phys. Chem. Chem. Phys.* 6, 4754–4763.
- (29) Olesen, K., and Andréasson, L.-E. (2003) *Biochemistry* 42, 2025–2035.
- (30) Ishikita, H., Saenger, W., Loll, B., Biesiadka, J., and Knapp, E. W. (2006) *Biochemistry* 45, 2063–2071.
- (31) Sproviero, E. M., Gascon, J. A., McEvoy, J. P., Brudvig, G. W., and Batista, V. S. (2008) *Coord. Chem. Rev.* 252, 395–415.
- (32) Hundelt, M., Hays, A. M. A., Debus, R. J., and Junge, W. (1998) *Biochemistry* 37, 14450–14456.
- (33) Phillips, J. C., Braun, R., Wang, W., Gumbart, J., Tajkhorshid, E., Villa, E., Chipot, C., Skeel, R. D., Kale, L., and Schulten, K. (2005) *J. Comput. Chem.* 26, 1781–1802.
- (34) Song, Y. F., Mao, J. J., and Gunner, M. R. (2009) *J. Comput. Chem.* 30, 2231–2247.
- (35) Song, Y. F., and Gunner, M. R. (2009) *J. Mol. Biol.* 387, 840–856.
- (36) Pokhrel, R., McConnell, I., and Brudvig, G. W. (2011) *Biochemistry* 50, 2725–2734.